DEFECT DETECTION ON HARDWOOD LOGS USING LASER SCANNING

Liya Thomas
PhD Student
Department of Computer Science

Lamine Mili
Professor
Department of Electrical and Computer Engineering
Virginia Tech
Blacksburg, VA 24061

Edward Thomas
Research Computer Scientist
USDA Forest Service, Northeastern Research Station
241 Mercer Springs Rd.
Princeton WV 24740

and

Clifford A. Shaffer[1]
Associate Professor
Department of Computer Science
Virginia Tech
Blacksburg, VA 24061

(Received August 2005)

ABSTRACT

To improve the sawyer's ability to process hardwood logs and stems, and thereby generate a higher valued product, automated detection methods of external defects have been developed and successfully tested on a large collection of real log samples. Since external defects provide hints about internal log characteristics, the location, type, and severity of external defects are the primary indicators of overall hardwood log quality and value. Using a high-resolution laser log scanner supplied by Perceptron, 162 red oak and yellow-poplar logs were scanned and digitally photographed. By means of 2-D circles fitted using a robust estimation method, a residual image is extracted from the laser scan data. Other robust fitting methods, such as ellipse and cylinder fitting, also are examined and their performance is evaluated. Our investigation reveals that the residuals, which are defined as the radial distances between the data points and the fitted curves or surfaces, provide valuable information about defects exhibiting height differentiation from the log surface. In other words, the log "skins" in the residual images show most bark texture features and surface characteristics of the original log or stem. Based on the contour levels estimated from a residual image, the developed methods allow us to detect most severe defects using a combination of simple shape definition rules with the height map. Less significant, yet severe defects are pinpointed using a shape profile.

Keywords: Computer vision, defect detection, robust estimation method, scanning log laser.

INTRODUCTION

Over the last few decades a broad variety of scanning technologies have emerged for wood processing. Several scanning and optimization systems are on the market that aid in the sawing of logs into lumber. Among them are defect detection and classification systems for logs and stems. Defect detection on hardwood trees and logs is categorized into internal and external de-

[1] The authors are, respectively, doctoral student, Department of Computer Science, and Professor, Department of Electrical and Computer Engineering, Virginia Tech, Blacksburg, VA 24061; Research Computer Scientist, USDA Forest Serv. Northeastern Research Station, 241 Mercer Springs Road, Princeton, WV 24740; and Associate Professor, Department of Computer Science, Virginia Tech, Blacksburg, VA 24061. The authors thank the USDA Forest Serv. Northeastern Research Station for partially funding this research, and Perceptron, Inc. for lending their laser scanning equipment for log data collection.

tection. Internal detection determines defects inside logs, while external detection identifies defects on a log's surface. Currently, most available scanning systems are external methods that use a laser-line scanner to collect rough log profile information. These systems were typically developed for softwood (i.e., pine, spruce, fir) log processing and for gathering information about external log characteristics such as diameter, taper, curvature, and length (Samson 1993). Once log shape data are obtained, a previously generated cutting pattern or template is selected that best fits the log. Optimization systems then use this profile information to better position the log on the carriage with respect to the saw and to improve the sawyer's decision-making ability. Adding external defect information to the optimization process is a natural extension of current technology.

While the various internal defect inspection methods proposed in the literature are based on X-ray/CT (Computer Tomography), X-ray tomosynthesis, MRI (magnetic resonance imaging), microwave scanning, ultrasound, and enhanced pattern recognition of regular X-ray images (Guddanti and Chang 1998; Schmoldt 1996; Wagner et al. 1989; Zhu et al. 1991), no commercial installation of these methods is known to exist at this time. Using CT data, computer vision algorithms such as the feed-forward artificial neural-network classifier (ANN) developed by Li et al. (1996), are able to accurately locate and describe internal log defects. Under certain conditions, CT or MRI systems provide the CT scanning device (Bhandarkar et al. 1999). In addition, it is expected that the expense of X-ray/CT systems would prevent their installation in many sawmills—particularly small- to medium-sized mills. Further, it would be easier and less expensive to install and maintain an external laser scanning system than an X-ray/CT system, based on the complexity of the latter system. External laser scanning systems have the potential to significantly improve the volume and value of boards produced and avoid the drawbacks of X-ray/CT and similar systems.

Traditionally, before a hardwood log is sawn, an assessment of its quality is performed, typically via a mill operator's visual inspection. This inspection process is quite subjective since it depends entirely on the operator's judgment and abilities. The presence and location of defects decrease log quality and value. In fact, the difference between high and low quality logs is determined by defect type, frequency, size, and location. While log defects are classified as external or internal defects, they are strongly related to each other since external defects typically stem from internal ones lying beneath them, down to the wood pith. Consequently, the former may be considered as external indicators of the latter. They consist of bumps, splits, holes, and circular distortions in the bark pattern. Bumps usually indicate overgrown knots, branches, or wounds. Some bumps have a cavity or hole in the middle, indicating that the overgrown material has turned rotten. Circular distortions, or rings around a central flattened area, indicate a branch that was overgrown many years or decades ago. Surface defects progress from a pruned branch, naturally or purposefully pruned during management, to an overgrown knot characterized by a significant bump, then to a rotten knot or a distortion defect, depending on the circumstances.

Studies have demonstrated that the use of external or internal defect data improves cutting strategies that optimize log recovery or yield, i.e., preserving the largest possible area of clear wood on a board face. The value of lumber that can be recovered depends on the presence and location of defects. This is especially true for hardwood logs. Softwoods are sawn to fixed stock dimensional sizes, e.g., 2 in. thick × 4 in. wide × n ft long (2×4s), 2 in. thick × 6 in. wide × n ft long (2×6s), etc. Normally little attention is paid to the placement of defects inside or on the log surface in softwood processing. However, in the production of hardwood lumber, boards are sawn to fixed thicknesses and random widths. The presence and placement of defects on the boards are of particular concern as they impact board quality and value. Therefore, much attention is given to the presence of log surface defects during processing. The use of a scanning system to detect log surface defects would im-

prove decision-making when the log is sawn into boards. This can be accomplished with a simple video system that displays the log to be processed along with its defects. The time needed to visually inspect logs would be minimized and enables the sawyer to detect defects that otherwise might be overlooked.

It is difficult to accurately and quickly detect and measure defects by either mechanical or manual methods (Tian and Murphy 1997). However, the potential value and yield gains associated with accurate automated defect detection are significant. In Steele et al.'s study (1994), 12 red oak logs were collected and divided into two groups that were as closely matched as possible with respect to log size and quality. Logs from one of the groups were sliced into 0.25-in. thick disks and the location and size of all defects were recorded. The data from the slices were assembled to create virtual logs showing all exterior and interior defects. The logs from one group were sawn to the best of a sawyer's ability to produce the highest valued lumber possible. The logs in the other group were sawn by computer using the available defect information. The logs sawn using the defect information averaged 11.21% higher value than those sawn manually without defect information.

Our research is focused on developing a cost-effective and reliable method of locating external defects on log surfaces (Thomas et al. 2004). To accomplish this, we employed a commercially available TriCam scanning system with four laser units (Perceptron 1999). This scanner generated high-resolution profile images of the log surface in three dimensions. The developed method consists of the following steps. First, the three-dimensional log surface image is processed to determine the location of the most severe defects, which include overgrown knots, rotten knots, holes/gouges, and removed branches. These types of defects usually are associated with a significant surface rise or depression depending on the defect type. The image is processed using a robust statistical approach to fit a series of circles to the log data. By analyzing the radial distances, defects characterized by a height change from the surrounding log area can be located. Another process is to locate defects that are severe but not as easily identified as the former. This is achieved through the examination of log surface data and the pattern matching of data segments to a predetermined defect profile.

In this paper we first describe the method we used for scanning logs. Then we present robust curve-fitting procedures for estimating log shape, a preliminary step for our defect detection method. We then generate a 2-D residual image from the curve-fitting process. Next we characterize and catalog the features of severe external defects on hardwood logs, which is used as input to the defect detector. In the final section, we present conclusions and plans for future work.

Description of the laser log scanning systems being used

A portable, demonstration laser log scanner by Perceptron, Inc. was used to collect the log surface data (Perceptron 1999). The scanner comprises four laser-line generator/camera units stationed at 90-degree intervals around the log's circumference. The scanner utilizes triangulation to determine locations of log surface points covered by the laser-line. The log stands still while the carriage holding the four scanning units moves on rails along the log's length. The logs are maintained in position by supports at 4-ft intervals.

The log scanner scans a 16-ft-long log at low resolution in less than 10 s and is designed to collect gross profile information. At low resolution a scan line around the circumference of the log is taken every 4.0 in. To achieve higher resolution, the speed at which the scanner moves along the log was slowed to approximately 15 ft per min. The slow scanning speed is a result of slowing the motors that move the scanning apparatus along the log. This is the only means available for us to increase the density of scan lines. A more elegant, but unavailable, solution would be to reprogram the system to take more frequent scan lines. At this speed a laser-line measurement is recorded approximately every

0.78 in. (Fig. 1). A transducer records the lineal position of the scanner accurate to 0.01 in. The data set shown in Fig. 1 consists of 1,290 three-dimensional Cartesian coordinates in a single plane. We refer to such a data set as a "cross-section." Depending on the circumference of the log at any specific location, the number of points in each cross-section varies. However, on average the distance between points in each cross-section is 0.04 in. When a sequence of cross-sections is assembled, a three-dimensional map of the log surface is obtained (Fig. 2). An additional computer program has been developed using OpenGL to render realistic views of the scanned log surfaces (Fig. 3). This program is especially useful for visually examining the logs and comparing detected defects with both the visible and manually recorded defect locations.

A combination of 162 northern red oak (*Quercus rubra*) and yellow-poplar (*Tulipifera liriodendron*) logs were scanned. These are two of the more common and important commercial species in the eastern United States. The sample of logs scanned is obtained directly from the forest and from local sawmills. In general, the logs from the forest are in better condition than those from sawmills. Because of less handling, the forest logs show less damage and have fewer and smaller areas of missing bark than the mill logs.

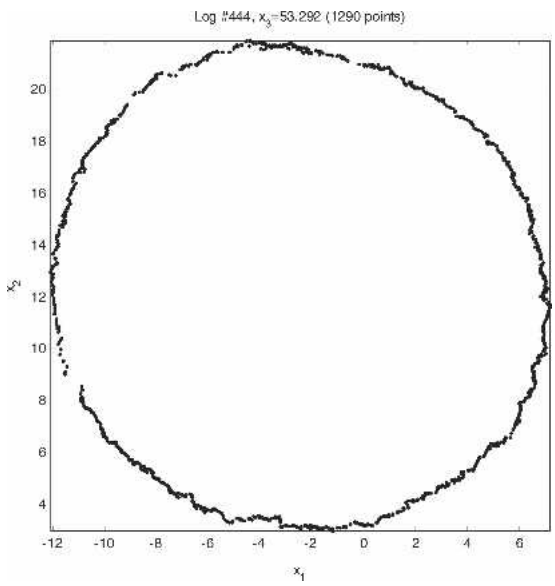

FIG. 1. A data cross-section representing the circumference of a log on a 2-D plane.

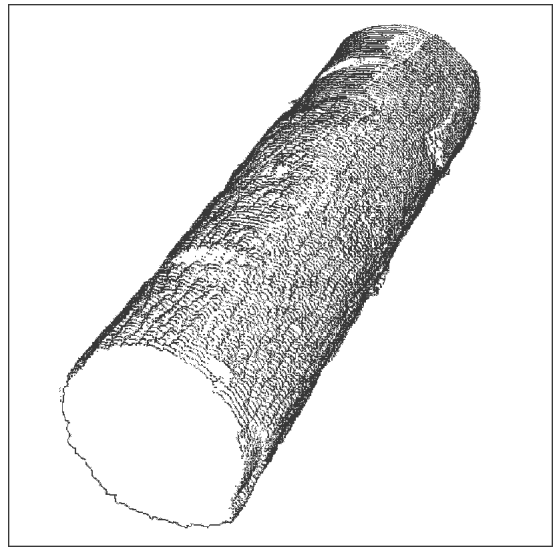

FIG. 2. Three-dimensional projection of the laser-scanned log data.

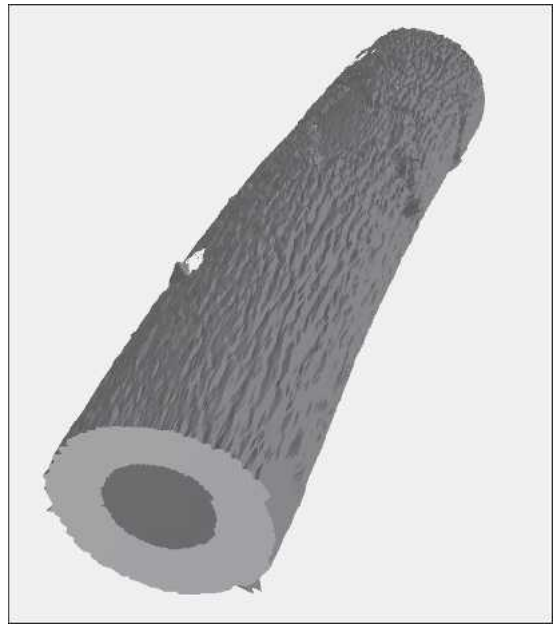

FIG. 3. OpenGL rendered image of the log data presented in Fig. 2.

A robust defect detection method based on range data provided by a laser scanner

Severe external defects that correspond to rises or depressions on the log surface can be observed from the three-dimensional log surface image. This suggests that one way to determine their location is to extract the height change on the log surface from its 3-D image. To do so, we apply a series of circle fittings to log cross-section data sets to obtain ground zero reference levels of the log surface. Because the range laser data sets may include either missing data or irrelevant deviant data points, we develop a new, robust estimator to estimate in a reliable manner the centers and the radii of the fitted circles. Radial distances between the latter and the log data points are thus indicative of the local height changes. Defects characterized by significant (in a statistical sense) surface rises or depressions are then located using appropriate statistical methods that are described next.

Circle fitting and outlier suppression

To convert the 3-D log surface data to 2-D images for processing, a reference surface must be imposed on the log data from the scanner. Since logs are natural objects that are approximately circular or elliptical along the cross-sections, we decided to experiment with fitting circles and ellipses to the log data, which all together form a reference surface, or virtual log, needed for defect detection. It turns out that defects that correspond to rises or depressions on the log surface can be detected using contour levels estimated from the orthogonal distances between the virtual log surface and any point of the cross-section.

Fitting quadratic curves (i.e., circles, ellipses) to 2-D data points is a nonlinear regression problem (Gander et al. 1994). Classic least-squares fitting methods fail in our case because the laser log cross-section data contain either missing data and/or large deviant data points, termed outliers in the statistical literature. These data characteristics are caused by both the logs and the scanning system. As depicted in Fig. 4, the laser data sets include deviant data generated by dangling loose bark, duplicate and/or missing data caused by scanner calibration errors, unwanted data from the supporting structure under the log, and missing data due to the blockage of the log by the supporting structure. In robust statistics, outliers are defined as data points that strongly deviate from the pattern formed by the majority of the measurements. To overcome the non-robustness of the least-square fitting, we resort to the theories and methods of robust statistics (Hampel et al. 1986). The nonlinear form of the circle equation prompts us to develop a new, robust estimation method that is an outgrowth of the one proposed by Mili et al. (1996).

Our nonlinear regression circle-fitting estimator is a generalized M-Estimator termed GM-Estimator for short (Thomas et al. 2004). As shown in Fig. 5, it filters out not only the errors in the measurements, but also the errors in the circle model that is applied to a given cross-section data set. For example, for a log sample with 120 cross-sections, an equal number of circles are fitted, forming a virtual log for the residual extraction as depicted in Fig. 2. Unlike the method described in Mili et al. (1996), our estimator minimizes an objective function that makes use of a weight function that levels off for large-scaled radial distance between the associated data point and the fitted circle; it does this at every step of the iterative algorithm that solves the estimator. The robust measure of the scale of these distances is performed by means of projection statistics (Mili et al. 1996; Rousseeuw and Van Zomerman 1991) while the minimum of the objective function is found through the iteratively re-weighted least-squares algorithm (Mili et al. 1996). For detailed information regarding our robust circle-fitting GM-Estimator, refer to Thomas et al. (2003).

To check that our nonlinear circle-fitting GM-Estimator is robust against outliers, we derive its influence function, which is a measure of the estimator's sensitivity to data contamination (Hampel et al. 1986). If this function increases without bounds as a data point is moved farther and farther away from its true value, the estimator is said to be non-robust; otherwise it is said

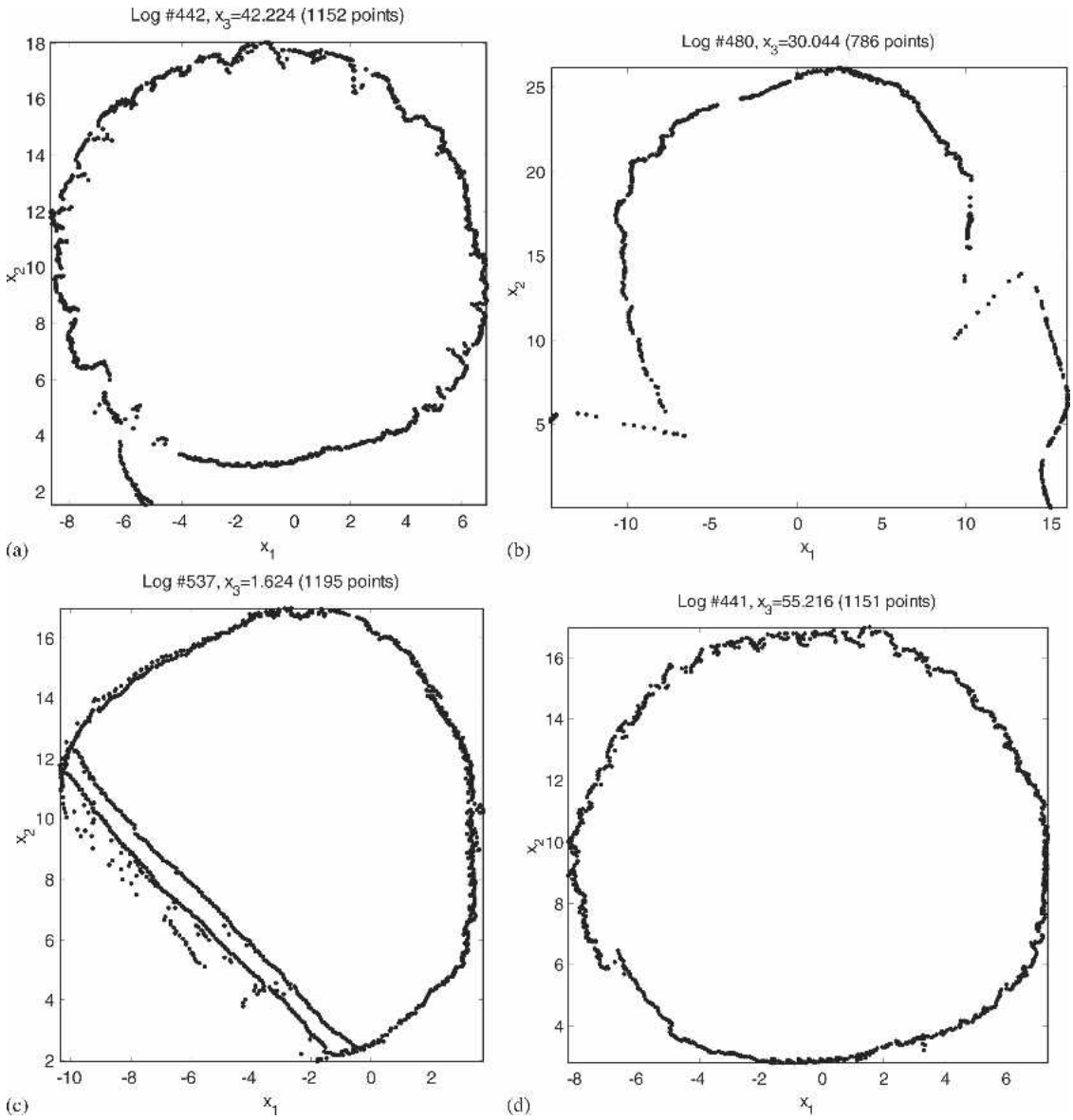

FIG. 4. Various formations of outliers present in cross-section data from laser scanning: a: loose bark flakes in lower left corner. b: outliers in form of scanning support structure and missing data due to structure. c: outliers and shape of log at one end where the log was cut diagonally instead of squarely. d: a good log data cross section containing no outliers.

to be robust. It can be shown that the influence function of our estimator can be decomposed as the product of two terms, one reflecting the influence of the model (i.e., the circle equation) and another reflecting the influence of the radial distances (i.e., the measurement errors). It can be shown that both terms are bounded, making our estimator robust against extreme outliers (Thomas et. al. 2004).

We tested the robustness of our estimator on real log data samples. It is found that the resulting fitted circles vary little among neighboring cross-sections, which yields a smooth fitting over the entire data of one log. Figure 5 displays

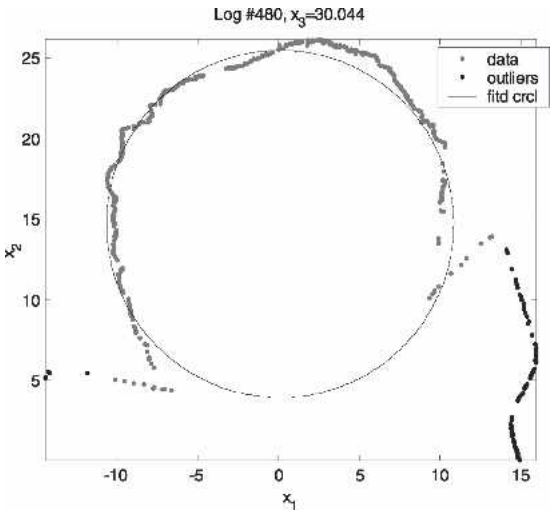

FIG. 5. Circle-fitting to a cross-section that contains a portion of the log support.

a circle that was fitted to a cross-section with a non-negligible fraction of outliers and missing data. Outliers identified by this method are plotted in bold. The smoothness of the fitting is further reinforced by smoothing the parameters using a box filter (Haralick and Shapiro 1992). Note that approximately 3% of the points are labeled as outliers, and hence suppressed from the data set (Thomas et. al. 2004).

Robust ellipse and cylinder fitting

We also experimented with a linear ellipse-fitting GM-Estimator that incorporates the heteroscedastic errors in variables model (Leedan and Meer 2000). The advantage of ellipse-fitting is that it provides better results in certain situations, for example when the cross-sections are predominately elliptical rather than circular in nature. However, the ellipse model involves five parameters (two for the center point, two radii, and the orientation angle of the ellipse), as opposed to three for the circle (the center point x and y values, and the radius). In addition, the estimation of radial distances between the measurements and the ellipses requires the use of an iterative algorithm. All these difficulties make ellipse-fitting a less attractive option.

At the cost of greater model and computational complexity, we may choose to fit instead a cylinder or a conic to the entire set of log data at once. This fit provides a uniform surface of reference for generating the residual data. In general, such an approach does not work well as log shapes are not strictly cylindrical or conic. Furthermore, our sequence of circle fittings may be regarded as the fitting of a generalized cylinder (Marr and Nishihara 1975) in a discrete sense.

Generating the residual gray-level image

The next step is converting the three-dimensional laser-scanned Cartesian coordinates into a two-dimensional, 256 gray-level image (Fig. 6). In this process, the log surface is unrolled onto a 2-D coordinate space. In essence, this process creates a "skin" of the log surface representing the pattern of the log's bark along with the bumps and bulges associated with most defects. Using the adjusted, fitted circle to each cross-section, we calculate the radial distances between circle and log surface points, typically ranging from -0.5 to 0.5 in. The radial distances are scaled to range from 0 to 255 and mapped to gray-levels to create a 2-D image. Originally the log data are not in a grid format, so they are processed and interpolated linearly to fill any gaps between data points. The x_3 value in the 3-D data is the coordinate in the third dimension or the z-axis value, which is the position along the log's length. It is mapped to the 2-D image as the y value, given by a row number. The x value of the image, given by a column number, is calculated by scaling the angle of a cross-section's point from the center of the fitted circle.

If the desired image is to be 750 pixels wide, the scaling factor would be $750/(2\pi)$. On average, the size of an unrolled log output image is about 2 MB (megabytes), or 1,400×1,600 pixels at 1 byte per pixel. To save space and future processing time, the resolution of the output gray-level image from log-data unrolling is reduced. The Gaussian pyramid algorithm (Haralick and Shapiro 1992) is applied and a 5×5 win-

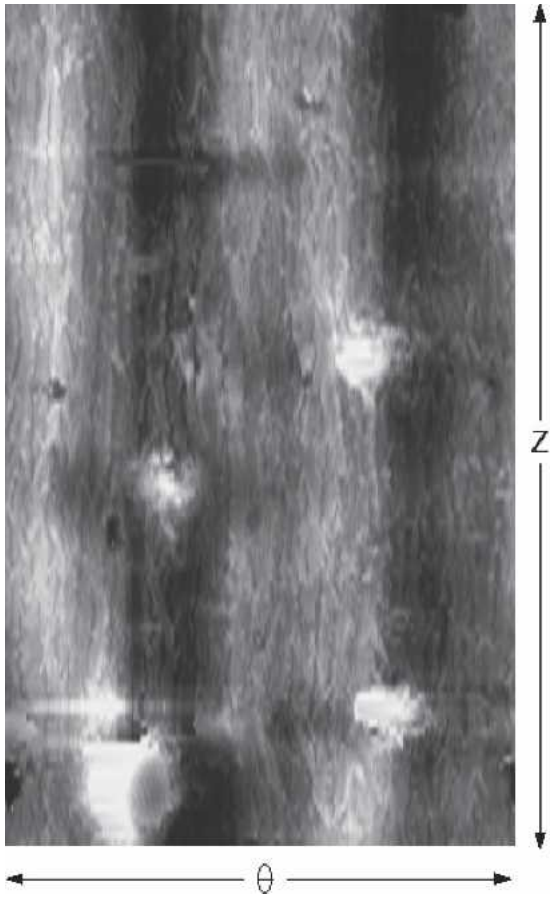

FIG. 6. Radial residuals generated by the log-unrolling processing presented as a gray-level image. Light pixels represent protrusions from the log surface, and dark pixels represent depressions. This log is approximately 9 feet in length with a diameter of 21 inches. The Z dimension is along the log's length. The Θ dimension is around the circumference of the log.

dow is used to smooth and sub-sample the image. The image is reduced to 25% of the original size, i.e., roughly 500 KB/image. This speeds additional analyses of the image with little or no loss of data of interest.

External defect characteristics

The residual images provide a solid foundation for detecting and classifying external log defects. Robust clustering and pattern recognition methodologies were employed for this purpose. An important part of a clustering and classification system is its training using sufficient, typical samples having unique object features. Once the system is well trained, it can identify an object and classify its type at a desirable classification rate. In our case, the objects are external log defects. Thus, we study about 200 medium to severe defect samples of red oak and yellow-poplar. Our goal is to better define and characterize external defect types of hardwood species from the conventional forest industry perspective; to extract features unique to each defect type; and to categorize external defect types discernible using the 3-D laser data. Loose bark on the log surface is not a defect. However, it tends to introduce outliers in our 3-D log data. Thus a sample collection of loose bark is studied as well. Table 1 lists three of the defect types that we studied.

The features examined include width along the log cross-section, length along the log length, the surface rise, and the surface depression. Each defect is measured manually and photographed using a high-resolution Nikon CCD digital camera. The sample measurements are analyzed for each defect type. Log curvature and slope along both the width and length directions are approximated. Statistics for each defect type including the average, median, first- and third-quartiles also are determined. We intend to use these data to help in modeling the features of each defect type that set it apart from others in the n-dimensional feature space, so that defects can be classified using a robust clustering and classification tool. Figure 7 displays photographs of two defects, while Table 2 lists their sample measurements and calculated feature values. The left two photographs are the side- and top- view of an overgrown knot on a red-oak log, respectively, and the right ones, a sound knot on a yellow-poplar.

Table 3 presents our study results from the defect samples. For example, the median width of overgrown knots is 5.5 in., smaller than that of sound knots, 6.5 in. Meanwhile, the median length of overgrown knots is 6.5 in., also smaller than that of sound knots, which amounts to 9.5 in. Thus we conclude that, in general, overgrown

TABLE 1. *The code, name, indicator, and definition of three external defect types.*

Defect code	Defect name	Surface rise (in.)	Indicator	Definition
OK	Overgrown knot	1.5	An abrupt surface rise, usually more than 0.5 inch, and texture change 2 to 8 inches in diameter.	A knot just below the bark surface.
SK	Sound Knot	1.0	Same as OK but characterized by a flat-sawn top.	Location where a branch was sawn from the log.
UK/RK	Unsound/Rotten knot	1.0	Often has a surface rise with a depression or hole in the middle, usually greater than 0.5 inches.	An overgrown knot or sound knot with a portion rotten.

knots are smaller than sound knots in terms of defect area size.

Traditionally by forest industry convention, if a sawn knot is not rotten, then it is referred to as a sound knot. On the other hand, if an overgrown knot or a sawn knot is rotten, then it is grouped into a third type, known as unsound knot. The laser-scanned data do not provide sufficient information to distinguish defects that are rotten or otherwise; thus our algorithm will not be able to classify them as well. For defect classification using laser data, we propose to regroup these three defect types, overgrown knots, sound knots, and unsound knots, into two new types which we call knobs and sawn knots. Knobs comprise all overgrown knots, regardless of whether they have decay; similarly, sawn knots include both sound and rotten ones. As is done for the defect types according to forest industry convention, we obtain statistics of the defect samples under the two corresponding new proposed categories.

Simulation results and discussion

To accommodate the countless possible defect sizes, heights, shapes, types, etc. in the 3-D log data, we developed an expert system to implement the defect detection task. The current version of our system uses the contour image generated from the radial distances, which provides a map of defect height change against the surrounding bark. Also used are the measured 3-D log data. Expert knowledge and expertise are applied in a stepwise fashion to rule out areas as potential defects, including areas in sizes smaller than a given threshold, nested in other curves, or long and narrow (determined by the "actual" width-to-length ratio, referred to as w/l for short). By "actual" we refer to the width-to-length ratio acquired through the calculation of the statistical medium of the widths of the area enclosed in the selected contour curve. The data resolution (0.8 in. per cross-section) and the nature of external defect shapes restrict search scope in the algorithm.

The algorithm attempts to find the most obvious defects based on their external characteristics, such as protrusion on surface, certain width-length ratio, and area size. These defects have a relatively significant high change on the surface ($\geq$0.5 in.), and/or a relatively significant size ($\geq$3 in. in diameter). We refer to such defects as "expected to be detected," while the other defects, less significant in size, are termed "unexpected to be detected" as illustrated in Table 4. Using the gray-level image shown earlier in Fig. 6, the algorithm generates a contour plot as depicted in Fig. 8, and determines the rectangles enclosing areas with a contour curve at the highest level. Then some areas are selected if they are big enough or with a significant height. In Fig. 8 four out of the nine surface defects are found using this method. Figure 8 also shows a manually recorded map of the defects on the same log. The defect types detected by our method in the map include SKC's (sound knot clusters), SK's (sound knots), and OK's (overgrown knots). Minor defects we did not expect to be detected include AK's (adventitious knots), AKC's (adventitious knot clusters), LD's

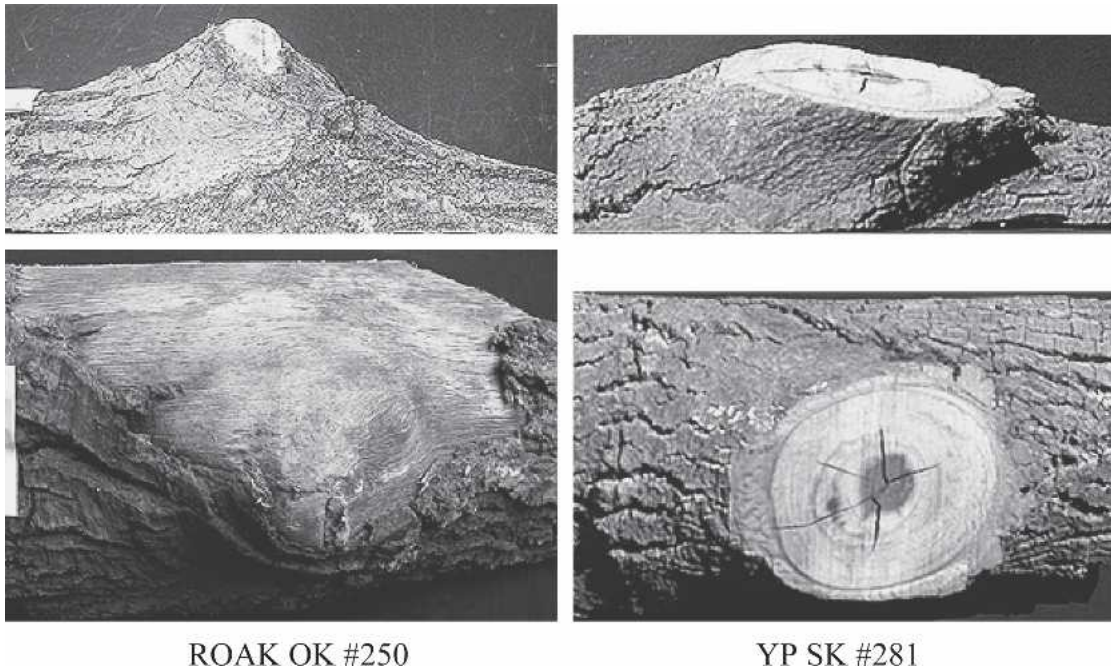

FIG. 7. Photographs of two external hardwood log defects. Left, overgrown knot (OK) on red oak; Right, sawn knot (SK) on yellow-poplar.

TABLE 2. *Measurements and feature approximation of the defects in Fig. 8.*

Specie	Type	#	Width (in.)	Length (in.)	Surface rise (in.)	Curvature along w.	Curvature along l.	Slope (°) along w.	Slope (°) along l.
ROAK	OK	250	7.5	9.5	2.5	0.36	0.22	48	58
YP	SK	281	6.5	10	2	0.38	0.16	52	66

TABLE 3. *Statistics of the measurements and feature approximations for three defect types. Each entry consists of the first-quartile, median, and the third-quartile of the sample measurements.*

Measurement	Defect types Overgrown knot	Sound knot	Unsound knot
Width (in.)	4.5–5.5–6.5	5.5–6.5~7.5	1.0–1.5–1.5
Length (in.)	5.50–6.50–7.50	6.60–9.50–12.40	6.30–7.50–9.50
Surface rise (in.)	1.00–1.50–1.50	0.60–1.00–1.50	0.90–1.00–1.50
Surface depression (in.)	–	0.80–1.00–1.50	0.90–1.00–1.50
Curvature along width	0.25–0.33–0.40	0.11–0.16–0.33	0.19–0.22–0.28
Curvature along length	0.17–0.22–0.28	0.06–0.09–0.16	0.13–0.16–0.19
Slope along width	55–64–69	61–71–74	64–69–73
Slope along length	63–66–69	73–77–81	68–73–76

(light distortions), and MD's (medium distortions).

Further, our algorithm includes a statistical expert system to examine the area surrounding a selected small region for relatively straight line segments. If the coverage of straight line segments is sufficient, the defect area is adjusted to cover the entire defect surface, rather than just a

TABLE 4. *Statistics of the simulation of our defect detection system.*

Defect type \ # of Defects to be detected	Expected		Unexpected		Grand Total		
	Total	Detected	Total	Detected	Total	Detected	False
Knobs	32	27	34	6	66	33	
Sawn knots	19	19	19	2	38	21	
Others	8	1	50	3	58	4	
All types	59	47	103	11	162	58	14

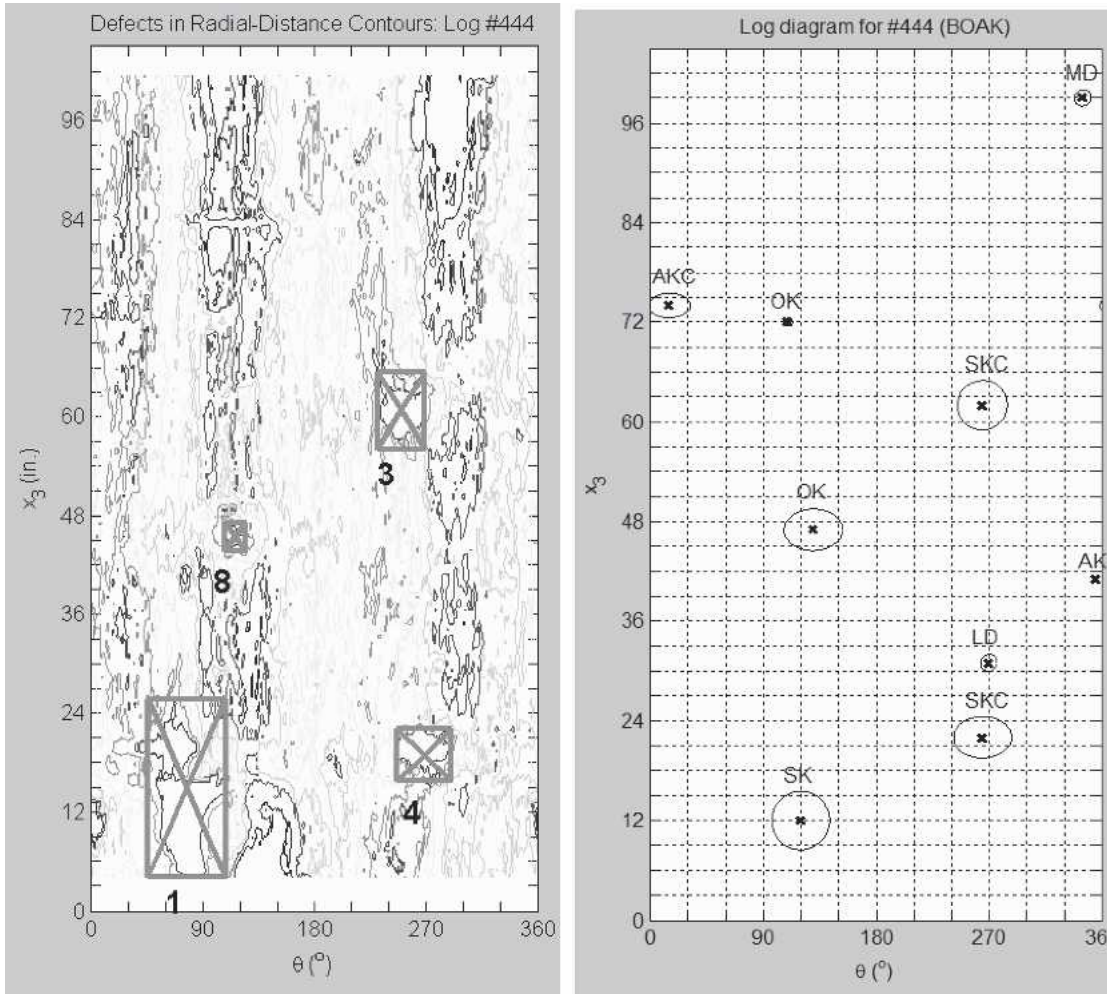

FIG. 8. Left: Contour plot of a log surface with the four most obvious defect areas marked with crossed rectangles labeled in the descending order of area size. Right: Defect diagram illustrating the "ground truth." Note that only five small and/or flat defects were not detected. Both plots were automatically generated by our Matlab programs.

corner. The algorithm examines angle changes between the lines connecting log data points along cross-section at certain intervals. If the changes are small enough ($\leq 25°$), the corresponding segments are recorded as nearly straight. Then the coverage of the "straight" segments is determined. If there are a sufficient number of straight segments, this area is identi-

fied as a flattop, which is likely a sawn top, either sound (not rotten), or unsound (rotten). Wrap-around areas refer to areas whose left border starts at the right side of the contour plot (~2π radians), and right one ends at the left side (~0 radians). To deal with these areas, all the corresponding data identified by their x, y, and z coordinates along with the borders of the areas are rearranged via calculation, rotation, and array shifting, so that the areas to be examined are centered at π radians. The previously wrapped-around areas can then be examined like other areas.

Log-surface defects come in many types, sizes, and shapes: knots, bumps or bulges, circular distortions, surface rise, and splits, to name a few. Knots include overgrown, adventitious, sound, or unsound (rotten). Distortions can be heavy, medium, or light. Knots can occur in clusters of various numbers and sizes. Approximately 60% of the severe defect types, including overgrown knots, rotten knots, bumps, sawn-off or removed branches, splits, and holes, have a height change, either a protrusion or a depression, of at least 0.5 in. when compared to the neighboring bark area. Other defects do not change much in terms of height. Some defects are easily identified by color or height characteristics. Others are not obvious except for their breaking of the natural bark pattern, i.e., a change in bark texture. In log processing, some types of defects are considered severe, such as knots and heavy distortions, while others are not as serious. Based on these observations, the data are processed such that log areas unlikely to contain defects can be ignored and removed from the foreground region.

Many severe defects are associated with a localized height change: a height analysis of the residual image provides information about the presence of such severe defects. A substantial, localized, and abrupt surface rise or depression greater than 1.0 in. is almost always a defect. The reason we chose 3 in. as the threshold for defect diameter is that the log-data resolution—0.8 in. per cross-section—is not high enough to well capture defects whose diameters are smaller than that. Since the pixel values in the gray-level image represent radial distances between the fitted circle and the log surface, the analysis is straightforward. In the contour plot image, it is possible to discern the areas containing likely defects based on height information alone.

Area-removal rules comprise: areas smaller than a given threshold are mainly tiny fragments; areas enclosed in curves nested in other curves are removed, as there will only be up to one defect in the same location; those being long and narrow are normal bark areas; areas that are smaller than 50 $in.^2$ and are too close to the selected large ones. Some areas are removed for further consideration if they contain a severe portion of missing data. Although not illustrated in Fig. 8, certain defects, in particular the sawn ones, are often detected partially in the contour. This is because they are relatively low-lying and flat, and often only a small portion of a sawn knot, e.g. a relatively high-raised corner, is enclosed in the highest contour. The algorithm adjusts the boundaries of this type of identified areas. Areas may include elevated yet non-defective log surface. Typically they are covered with tree bark, thus associated with distinctive bark patterns. Finally, due to the lack of "depressed" defect samples in the log data, at this stage of development our system does not detect such defect types.

Table 3 presents statistics for the simulations of our defect detection system. Fifteen log samples were randomly chosen containing 162 surface defects in total. The detection system does not classify the type of defects, e.g., overgrown knots, unsound knots, sawn knots, etc. Instead, the classification is done manually through our examination of the detection results including the contour plots, the defect diagrams (ground truth), gray images, and the colored log photos. The last row of the table, excluding the value in the last column, displays the sums of the data in each column. The program made a total of 72 predictions of defects. It correctly identified 47 of 59 "expected" defects, 11 of 103 "unexpected" ones, and incorrectly predicted 14 locations as defects. Note that as a future research work, a method that makes use of the gray-level information provided by the residual image will

be developed to further enhance the defect detection tests of the "unexpected" category.

CONCLUSIONS AND FUTURE WORK

This paper describes our approach for detecting surface defects in hardwood logs. Because of the presence of extreme outliers and missing data in the laser log data set, robust estimation techniques are well suited to this application. The developed programs can process an entire log-data sample by transforming the original log data set, which may contain a large number of missing and/or severe deviant data, into a sharper and cleaner image. The quality of the resulting gray-level image lays a solid foundation for the remaining defect-detection process. It is found that contour levels derived from the residuals make it possible to detect and further narrow down the potential defect areas. For defects that lie within the bark layer, the pixel information of the gray-level image needs to be utilized; this calls for further research and development.

When a single cylinder is fitted to the entire log data, the number of parameters to be estimated is the fewest as compared to fitting a sequence of circles and ellipses to all cross log sections. This means that cylinder-fitting provides the fewest degrees of freedom. In addition, the residuals are extracted against a uniform surface, resulting in the smoothest image among the three. In contrast, the circle-fitting approach involves far more parameters to be estimated, which results in more degrees of freedom. However, each circle provides a better fit to each individual cross-section, revealing more details on log surface while residuals extracted between neighboring cross-sections are less consistent, or noisier, than in the cylinder case. On the other hand, ellipse-fitting introduces the greatest number of estimated parameters and hence generates the most detailed residual image. By the same token, residuals from neighboring cross-sections are much less consistent, or less crisp, compared to the previous two cases.

The generation and initial processing of the residual image is not the final step of this work. Clearly, additional research is needed. At this point, only log unrolling and height analyses methods have been examined. A preliminary study was conducted to extract features of external defect types from randomly chosen defect samples. These features were used to train a robust clustering and classification system for the defect classification. Texture analysis methods will be investigated to detect defects without change. To reach the final goal of locating and classifying surface defects, we are exploring the potential benefits of image processing, computer vision, and pattern recognition techniques using residual data.

Disclaimer

The use of trade, firm, or corporation names is for the information of the reader. Such use does not constitute an official endorsement or approval by the U.S. Department of Agriculture, Forest Service, or the Virginia Polytechnic Institute and State University of any product or services to the exclusion of others that may be suitable.

ACKNOWLEDGMENTS

The authors thank the USDA Forest Serv. Northeastern Research Station for partially funding this research, and Perceptron, Inc. for lending their laser scanning equipment for log data collection.

REFERENCES

BHANDARKAR, S. M., T. D. FAUST, AND M. TANG. 1999. CATALOG: A system for detection and rendering of internal log defects using computer tomography. Machine Vision and Applications. 11:171–190. Springer-Verlag Berlin, Germany.

GANDER, W., G. H GOLUB, AND R. STREBEL. 1994. Fitting of circles and ellipses—least squares solution. Tech. Rep. 217, Insitiut fur Eisenschaftliches Rechnen, ETH Zurich. Available via anonymous ftp from ftp://ftp.inf.ethz.ch/doc/tech-reports/2xx/ .

GUDDANTI, S., AND S. J. CHANG. 1998. Replicating sawmill sawing with TOPSAW using CT images of a full length hardwood log. Forest Prod. J. 48(1):72–75.

HAMPEL, F. R., E. M. RONCHETTI, P. J. ROUSSEEUW, AND

W. A. STAHEL. 1986. Robust statistics: The approach based on influence functions. John Wiley, New York, NY.

HARALICK, R. M., AND L. SHAPIRO. 1992. Computer and robot vision. Vol. 2. Addison-Wesley Longman Publ. Co. Inc., Boston, MA.

LEEDAN, Y., AND P. MEER. 2000. Heteroscedastic regression in computer vision: Problems with bilinear constraint. Int. J. Computer Vision. 37:127–150.

LI, P., A. L. ABBOTT, AND D. L. SCHMOLDT. 1996. Automated analysis of CT images for the inspection of hardwood logs. Proc. Int. Conf. on Neural Networks, Washington, D.C. Volume 3:1744–1749.

MARR, D, AND H. K. NISHIHARA. 1975. Spatial disposition of axes in a generalized cylinder representation of objects that do not encompass the viewer. Memo No 341, Artificial Intelligence Laboratory, Massachusetts Institute of Technology, Cambridge, MA.

MILI, L., M. G. CHENIAE, N. S. VICHARE, AND P. J. ROUSSEEUW. 1996. Robust state estimation based on projection statistics. IEEE Trans. on Power Systems. Vol. 11. No. 2.

PERCEPTRON, FOREST PRODUCTS DIVISION. 1999. Url: http://www.usnr.com/perceptron/products.htm. Perceptron Inc., Farmington Hills, MI.

ROUSSEEUW, P. J., AND B. C. VAN ZOMERMAN. 1991. Robust distances: Simulations and cutoff values. W. Stahel and S. Weisberg, Directions in robust statistics and diagnostics, Part II, 195–203. Springer-Verlag, Berlin, Germany.

SAMSON, M. 1993. Method for assessing the effect of knots in the conversion of logs into structural lumber. Wood Fiber Sci. 25(3):298–304.

SCHMOLDT, D. L. 1996. CT imaging, data reduction, and visualization of hardwood logs. *In* D. Meyer, ed. Proc. 1996 Hardwood Res. Symp. National Hardwood Lumber Association, Memphis, TN.

STEELE, P. H., T. E. G. HARLESS, F. WAGNER, L. KUMAR, AND F. W. TAYLOR. 1994. Increased lumber value from optimum orientation of internal defects with respect to sawing pattern in hardwood sawlogs. Forest Prod. J. 44(3): 69–72.

THOMAS, E., L. THOMAS, L. MILI, R. EHRICH, A. L. ABBOTT, AND C. A. SHAFFER. 2003. Primary detection of hardwood log defects using laser surface scanning. IS&T/SPIE's Electronic Imaging 2003, 20–24 January 2003, Santa Clara, CA. Vol. 5011:39–49.

THOMAS, L., L. MILI, C. A. SHAFFER, AND E. THOMAS. 2004. Defect detection on hardwood logs using high resolution three-dimensional laser scan data, IEEE ICIP 2004, Singapore, October 24–27, 2004:243–246.

TIAN, X., AND G. E. MURPHY. 1997. Detection of trimmed and occluded branches of harvested tree stems using texture analysis. Int. J. For. Eng. Vol. 8, No. 2.

WAGNER, F. G., F. W. TAYLOR, D. S. LADD, C. W. MCMILLIN, AND F. L. RODER. 1989. Ultrafast CT scanning of an oak log for internal defects. Forest Prod. J. 39(11/12):62–64.

ZHU, D., R. CONNERS, F. LAMB, AND P. ARAMAN. 1991. A computer vision system for locating and identifying internal log defects using CT imagery. Proc. 4th Int. Conf. on Scanning Tech. in the Wood Ind., Miller Freeman Publishing, Inc., San Francisco, CA:1–13.